Rapid Field-Scale CO2 Storage Simulation Tool with Geomechanically Constrained Fault Leakage

Ramachandran, Hariharan; Musa, Ikhwanul Hafizi; Tan, Chee Phuat; Geiger, Sebastian; Doster, Florian

DOI
10.56952/IGS-2024-0782

Publication date
2024

Document Version
Final published version

Citation (APA)
Ramachandran, H., Musa, I. H., Tan, C. P., Geiger, S., & Doster, F. (2024). *Rapid Field-Scale CO2 Storage Simulation Tool with Geomechanically Constrained Fault Leakage*. Paper presented at International Geomechanics Conference 2024, Kuala Lumpur, Malaysia. https://doi.org/10.56952/IGS-2024-0782

Rapid Field-Scale CO_2 Storage Simulation Tool with Geomechanically Constrained Fault Leakage

Hariharan Ramachandran 1*
Institute of GeoEnergy Engineering, Heriot-Watt University, Edinburgh, UK
Ikhwanul Hafizi Musa & Chee Phuat Tan 2
PETRONAS Group Technology & Commercialisation, Kuala Lumpur, Malaysia
Sebastian Geiger 3
Department of Geoscience and Engineering, Delft University of Technology, Delft, Netherlands
Florian Doster 1
Institute of GeoEnergy Engineering, Heriot-Watt University, Edinburgh, UK
* Hariharan Ramachandran (h.ramachandran@hw.ac.uk)

ABSTRACT: Geological carbon dioxide (CO_2) storage is vital for climate change mitigation, but CO_2 leakage, particularly through faults, poses significant risks. Accurately simulating the impact of fault properties across scales is crucial for predicting field-scale CO_2 injection and storage outcomes. However, this task is challenging due to limited knowledge, data scarcity, and computational constraints. This study introduces a fast tool for CO_2 leakage risk assessment that addresses these challenges. The tool combines a vertically integrated reservoir model with an upscaled fault leakage function based on source/sink relations. It conceptualizes faults as zones of increased vertical permeability in the caprock and reduced horizontal permeability in the reservoir. A steady-state flow approximation estimates CO_2 leakage along faults. Geomechanical effects on fluid flow are modeled by coupling fault porosity and permeability, amongst several other parameters with effective stress using constitutive relations. A decoupled method based on Geertsma's uniaxial expansion coefficient, assuming zero lateral strain and constant total vertical stress is used here. Example simulations are shown to illustrate the impact of geomechanically constrained fault parameters such as capillary entry pressure and permeability on fault leakage. The fast model presented in this study is a valuable tool for identifying uncertainties in key fault parameters and other constitutive relations that affect the behavior of the storage reservoir and potential fault leakage outcomes.

1. INTRODUCTION

Geological carbon dioxide (CO_2) storage, particularly in saline aquifers, is essential for mitigating climate change (Krevor et al., 2023). These aquifers have substantial storage capacities, but successful implementation relies on secure containment of CO_2. Leakage poses risks to mitigation efforts and undermines public trust in Carbon Capture and Storage (CCS). Faults are critical in this context, as they can either act as structural traps that confine CO_2 or serve as leakage pathways (Knipe et al., 1998; Snippe et al., 2021). As CCS deployment increases, encountering faulted storage formations is inevitable. Faults are complex geological structures with a low-permeability core surrounded by a fractured damage zone, which can increase leakage potential (Fig. 1) (Rizzo et al., 2024). Fault leakage is influenced by various factors, including geometry, architecture, stress regime, and rock properties. Injection-induced changes can reactivate faults, potentially creating new leakage pathways. Sub-seismic fractures within damage zones introduce significant uncertainties in CCS operations due to limited understanding of their presence and properties.

The scarcity of fault data, especially during early project stages, hinders informed decision-making. As operators evaluate multiple storage sites, efficient screening methods are necessary to identify geologically suitable candidates. Reservoir simulation is essential for assessing

potential fault leakage rates, but detailed models are computationally intensive.

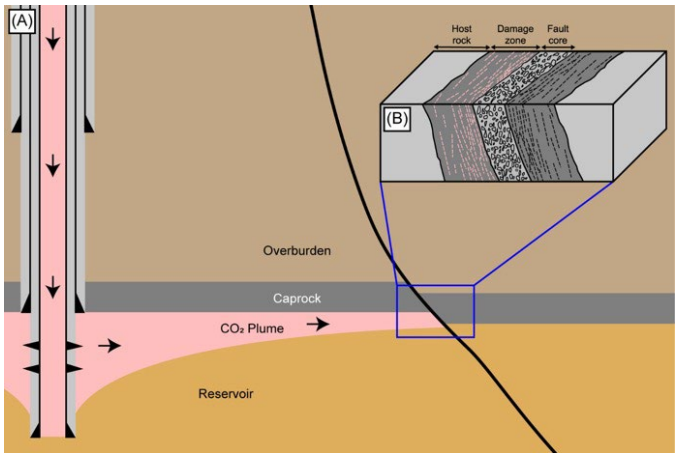

Fig. 1. This illustration depicts CO_2 storage in a geological system characterised by a faulted reservoir and caprock. The CO_2 is injected into highly permeable rock that can be several hundred metres thick, overlain by a regional seal of low permeability serving as the caprock. Faults present in this system can have dual effects: they may improve trapping or facilitate leakage, depending on their properties (A). The accompanying schematic (B) provides a detailed view of the fault zone structure, highlighting the fault core and damage zone. This figure is adapted from Gasda et al. (2022) and Ramachandran et al. (2024).

This paper presents a novel approach to model fault leakage by coupling a geomechanically constrained fault leakage function with a vertical equilibrium (VE) reservoir model. The method is implemented using MRST-co2lab, an open-source software package (Anderson, 2017; Lie, 2019). The fault is conceptualized as increased vertical permeability along the caprock and reduced horizontal permeability across the reservoir. The flow is simplified to single-phase flow along the fault, with rates estimated using Darcy's law, considering pressure differentials across layers, allowing for a 1D leakage system that reduces computational costs. This approach enables a more robust evaluation of storage potential while accounting for complexities and uncertainties in faulted geological settings, ultimately contributing to safer and effective storage practices.

2. METHODS

A vertically integrated reservoir-scale flow model is coupled with a geomechanically constrained upscaled fault leakage function for this purpose. A brief overview of the governing equations is presented in this section.

2.1. Reservoir Modelling

The 3D mass conservation equation for two immiscible and incompressible fluid phases α, CO_2 (α=g) and brine (α=w) turn into a volume conservation equation

$$\frac{\partial(\phi s_\alpha)}{\partial t} + \nabla \cdot u_\alpha = q_\alpha, \tag{1}$$

where s_α is the saturation of phase α, ϕ is the porosity, u_α is the Darcy velocity of phase α, and q_α is a source/sink term in units of volume of phase α per time. The porous medium is assumed to be a rigid medium under isothermal conditions. The volume balance is established by

$$s_g + s_w = 1. \tag{2}$$

The Darcy velocity is given by

$$\boldsymbol{u}_\alpha = -\frac{k_{r\alpha}}{\mu_\alpha}\boldsymbol{k}(\nabla p_\alpha - \rho_\alpha \boldsymbol{g}), \tag{3}$$

where $k_{r\alpha}$ is the relative permeability of phase α, μ_α is the viscosity of phase α, $\boldsymbol{k}$ is the permeability tensor, ρ_α is the density of phase α, p_α is the fluid pressure of phase α, and $\boldsymbol{g}$ is the gravity acceleration vector. The phase pressures are related by the capillary pressure function

$$p_c = p_g - p_w. \tag{4}$$

To obtain the fluid saturations and pressures by solving this system, three conditions must be met: firstly, specific functions must represent relative permeability and capillary pressure; secondly, initial conditions for pressure and saturation throughout the reservoir domain must be established; and thirdly, appropriate boundary conditions must be defined.

2.2. Vertical Equilibrium Modelling

In subsurface flow processes, the lateral dimension of interest is typically orders of magnitude larger (hundreds of metres to kilometers) compared to the vertical dimension (metres to tens of metres). This disparity leads to a rapid redistribution of fluids vertically, allowing for the approximation of VE (Nordbotten & Celia, 2011). As a result, the CO_2 forms a thin layer beneath the caprock, and the vertical pressure and fluid saturation distributions can be approximated by buoyancy and capillary forces. VE models reduce the dimensionality of the problem by vertically averaging the governing equations, which include conservation of mass and Darcy's law for fluid flow. This simplification results in a model that requires fewer grid cells and is computationally less intensive compared to full 3D simulations. Post-simulation, the vertical pressure and fluid saturations can be reconstructed from the set of upscaled variables obtained by vertically integrating the conservation equations. For a more general and in-depth treatments of the derivations and the limits of the VE assumption, the readers are referred to the relevant literature (Yortsos 1995; Nordbotten & Celia, 2011).

2.3. Upscaled Fault Leakage Function

This section details the steady-state analytical solution used to estimate leakage rates along the fault. The model

conceptualises the fault as a connection between the storage reservoir and a shallower secondary aquifer, which acts as a sink for leaking CO_2 (Fig. 2). The fault is represented by a low permeability core preventing across-fault flow, surrounded by high-permeability damage zones allowing vertical flow as shown in Fig. 2. The fault is hypothesised as an equivalent porous medium with appropriate properties describing it. Once the CO_2 plume reaches the base of the fault, it is hypothesized to form a thick layer, acting as a barrier for aqueous phase entry into the fault (Kang et al., 2014). As a result, the aqueous phase flux along the fault is considered negligible and excluded from the model.

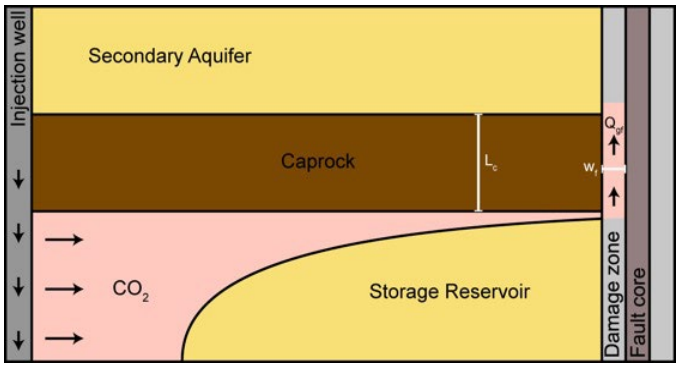

Fig. 2. A schematic representation of a vertical cross-section of a storage reservoir containing a fault. CO_2 leaks along the damage zone once it reaches the base of the fault within the reservoir. Figure adapted from Ramachandran et al., (2024).

The along fault leakage calculation is based on the model presented by Neufeld et al. (2009), that has been adapted to account for the reservoir overpressure caused by injection. This model describes leakage through fissures between two aquifers. We model the driving potential ψ as

$$\psi = \Delta\rho \boldsymbol{g} h_g + (P_w - P_{w0}) - p_e, \qquad (5)$$

where $\Delta\rho = \rho_w - \rho_g$ is the density difference between brine and CO_2, h_g is the height of CO_2 of the reservoir block connected to the fault block, P_w is the brine pressure in the reservoir, P_{w0} is the initial brine pressure in the reservoir, and p_e is the fault capillary entry pressure. CO_2 needs to overcome the fault capillary entry pressure for it to leak (Espinoza & Santamarina, 2017; Zheng & Espinoza, 2022). The vertical gas leakage flux Q_{gf} along the fault is given as

$$Q_{gf} = \begin{cases} 0, & \psi \le 0 \\ \dfrac{A_f k_f}{\mu_g} \dfrac{(\psi + \Delta\rho \boldsymbol{g} L_c)}{L_c}, & \psi > 0 \end{cases} \qquad (6)$$

where A_f is the area of the fault perpendicular to flow, k_f is the vertical fault permeability and L_c is length of the caprock or the length of the fault connecting the storage reservoir to the secondary aquifer. This approach relaxes the assumption of VE at the grid block where the fault is connected, allowing for non-zero vertical flow. However, for steady-state single-phase flow, fault leakage does not have a significant effect on reservoir predictions (Kang et al., 2014).

2.4. Simplified Geomechanical Modelling

The subsurface is treated as a poromechanical system where the mechanical behavior is modelled using equation of linear poroelasticity. A simplifying assumption of zero lateral strain and constant vertical stress is considered such that the mechanical displacement occurs exclusively in the vertical direction. This assumption reduces a 3D problem into 1D. Although this assumption may not be strictly applicable in all cases, it serves as a satisfactory approximation when dealing with relatively smooth pressure fields (Andersen, 2017). Furthermore, the mechanical displacement is neglected in the reservoir and assumed to affect only the fault for this model. The fault pore volume compressibility, c_ϕ, is expressed as

$$c_\phi = \frac{1}{K}(1-\alpha)\left(\frac{\alpha}{\phi_n} - 1\right) + \frac{\alpha}{\phi_n} c_m, \qquad (7)$$

where K is the bulk modulus, α is the Biot-Willis coefficient, ϕ_n is the new porosity, c_m is the Geertsma's uniaxial poroelastic expansion coefficient, expressed as $\frac{\alpha}{K_v}$ where K_v is the fault rock's uniaxial bulk modulus computed as $K_v = K + \frac{4}{3}G$ where G is the shear modulus. The new porosity, ϕ_n, is expressed as a function of pore volume compressibility as,

$$\phi_n = \phi_0\left[1 + c_\phi(p_n - p_o)\right], \qquad (8)$$

where ϕ_0 is the initial fault porosity at initial pressure, p_o and p_n is the new pressure at the fault-reservoir interface. The new permeability is evaluated using a Kozeny-Carmen based empirical relationship as

$$k_n = k_0\left(\frac{\phi_n}{\phi_i}\right)^3\left(\frac{1-\phi_i}{1-\phi_n}\right)^2, \qquad (9)$$

where k_0 is the initial fault permeability at pressure p_o and k_n is the new fault permeability at pressure p_n. The fault capillary entry pressure is expressed based on a Leverett J-function relationship as,

$$p_{en} = p_{e0}\sqrt{\frac{k_0\phi_n}{k_n\phi_0}}, \qquad (10)$$

where p_{e0} is the initial fault capillary entry pressure at pressure p_o and p_{en} is the new fault capillary entry pressure at pressure p_n.

3. RESULTS

The J area, a potential CO_2 storage site in the Malay Basin offshore Peninsular Malaysia is used to illustrate the

model presented in previous section. This matured hydrocarbon province, approximately 500 km long, 200 km wide, and 12 km deep, is considered for CCS due to its numerous mature fields and saline aquifers (Abd Rahman et al., 2022; Hasbollah et al., 2020). Located on the Northern margin, the target reservoir lies at a depth of 1984 m below the seafloor, which is at a depth of 70 m below sea level with the reservoir primarily consisting of Lower to Middle Miocene sandstones (de Jonge-Anderson et al., 2024b).

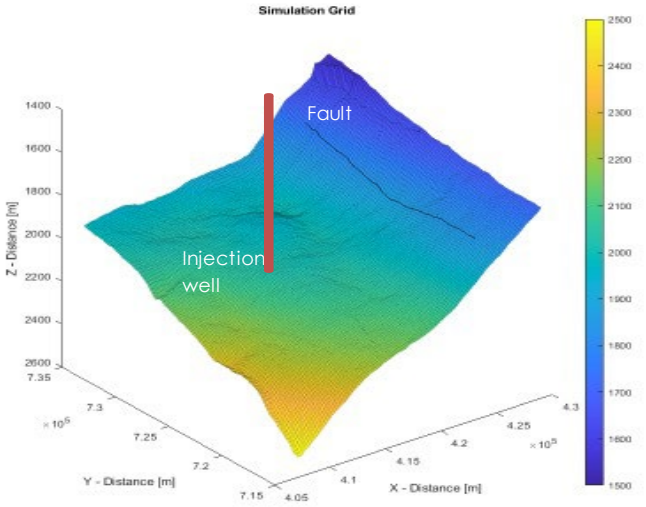

Fig. 3. Inclined 3D view of the reservoir showing the location of the injection well and the location of the fault. The target reservoir is at depth between 1500 – 2500 m below the seafloor.

Previous studies have identified the most suitable injection location for an injection rate of 1 Mt per year for 30 years followed by 970 years of migration at this basin (de Jonge-Anderson et al., 2024a; Ramachandran et al., 2024). The geothermal gradient is set at 50 °C/km, with a seafloor temperature of 24 °C (Madon & Jong, 2021). A 26 km-long fault is incorporated into the model, positioned 12 km from the injection well as shown in Fig. 3. The relevant reservoir and fault properties are listed in Table 1. The model boundaries are treated as open, with the pressure maintained at hydrostatic conditions. To simulate the presence of an impermeable fault core, the grid cells adjacent to the fault were adjusted to have zero cross-fault permeability. Additionally, a fault leakage function was integrated into these cells to account for fluid flow along the fault. This case study aims to evaluate the interplay of geomechanics and fault properties on along-fault leakage during CO_2 injection within the J area.

Numerical simulations were conducted to evaluate the impact of geomechanical constraints on fault permeability. Two sets of simulations, one incorporating geomechanics and another without were executed on an Apple MacBook Pro with the M1 chip, each completed in under 30 seconds. The simulations used identical initial fault capillary entry pressures across four fault permeabilities, with results presented in Fig. 4. At the conclusion of the 1000-year simulation for a fault permeability of 10^{-8} D, the total of 30 Mt of CO_2 was injected, with 100 t leaking along the fault, representing 0.0003% of the total injected. In the absence of geomechanics, fault permeability did not affect the onset of leakage (Fig. 4a), and the total leakage decreased following a power law trend with an exponent almost equal to 1 as fault permeability decreased (Fig. 4b). The exponent was less than 1 due to the balance in flow between lateral migration in the reservoir and vertical migration along the fault. However, when geomechanical constraints were included, leakage onset occurred earlier, and the leakage rate was higher compared to the scenario without geomechanics. The total leakage increased by 32% with the incorporation of geomechanical factors, underscoring its significance.

Table 1 – Summary of model parameters used for field-scale simulation described in Section 3. Adapted from de Jonge-Anderson et al., (2024a) and Ramachandran et al., (2024).

Property	**Value**
Reservoir description	
Number of cells (NX*NY*NZ)	100 x 110 x 5
Cell dimensions (DX*DY) (m)	200 x 200
Area (km^2)	440 (22 x 20)
Average top reservoir depth (m)	1984
Porosity	0.2
Permeability (mD)	50
Rock compressibility (Pa^{-1})	4.35×10^{-10}
Seafloor temperature (°C)	24
Temperature gradient (°Ckm^{-1})	50
Seafloor Depth (m)	70
Fluid properties (at 2000m depth)	
Brine viscosity (Pa.s)	3.13×10^{-4}
Gas viscosity (Pa.s)	3.21×10^{-5}
Brine density (kgm^{-3})	1001
Gas density (kgm^{-3})	389.7
Fault properties	
Fault permeability (D)	1×10^{-8}
Fault width (m)	10
Fault Porosity	0.01
Fault length (m)	500
Fault Capillary Entry Pressure (bar)	0.5
Fault Bulk Modulus (GPa)	10
Fault Shear Modulus (GPa)	1
Rock-Fluid properties (Brooks-Corey Model)	
Residual gas saturation	0.2
Irreducible brine saturation	0.25
Gas end-point relative permeability	1
Brine end-point relative permeability	1
Gas relative permeability exponent	1
Brine relative permeability exponent	1

The observed increase in leakage due to geomechanics can be attributed to several factors. When CO_2 reaches the fault downdip, it elevates the pressure at the reservoir-fault interface. This causes fault porosity and permeability to increase, while fault capillary entry pressure decreases, based on the empirical models in Section 2.4. Consequently, the increase in fault permeability results in a higher leakage rate, while the decrease in fault capillary entry pressure results in earlier onset of fault leakage.

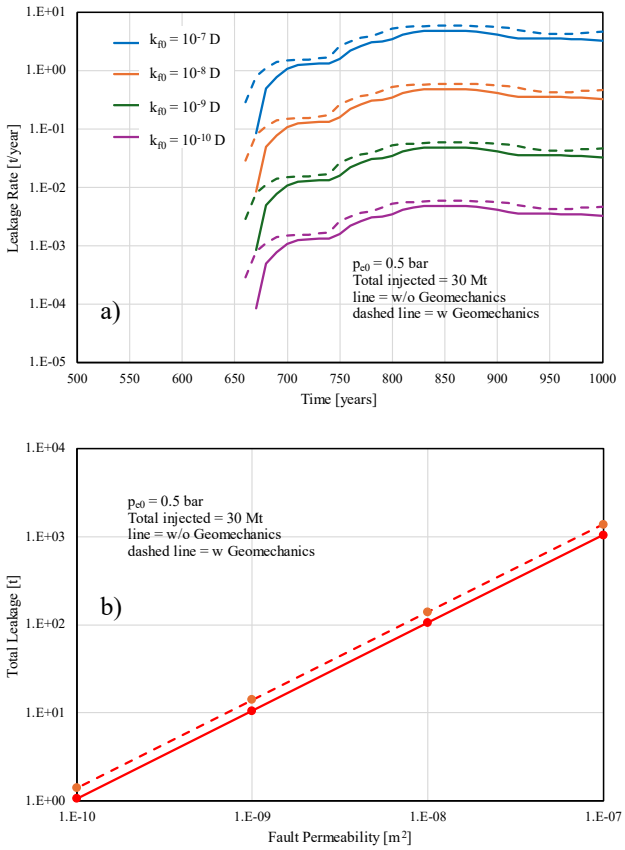

Fig. 4. Impact of fault properties on CO_2 leakage showing the relationship between fault permeability and the CO_2 leakage rate (a) and the decrease in total CO_2 leakage with decreasing value for fault permeability (b) for simulations with and without incorporating geomechanics.

Fault capillary entry pressure is a critical factor in assessing potential leakage scenarios with high values effectively preventing leakage even in permeable faults (Monzocchi et al., 2010; Zheng & Espinoza, 2022). To evaluate its impact, simulations with and without geomechanical constraints were conducted using increasing capillary entry pressures while maintaining other parameters constant (Table 1). Figs. 5a and 5b present the leakage rates and total leakage, respectively.

As fault capillary entry pressure increases, leakage rate decreases and onset delays. A pressure of 0.9 bar resulted in a fully sealing fault under the given injection conditions. For context, typical caprock and faulted rock capillary entry pressures range from a few to few tens of bars (Espinoza & Santamarina et al., 2017). Geomechanics had minimal impact on leakage onset for lower capillary entry pressures, with total leakage increasing by 4% and 14% for 0.0 and 0.25 bar capillary entry pressures, respectively. However, its effect was more pronounced at higher capillary entry pressures, with increases of 32% and 140% for 0.5 and 0.75 bar entry pressures, respectively. Although the percentage increase appears substantial for the 0.75 bar scenario, the absolute increase in total magnitude was less than 8 t. This analysis reinforces the importance of fault capillary entry pressure as a key constraint on leakage onset and rates in CO_2 storage scenarios, while also demonstrating the varying influence of geomechanical factors across different pressure ranges.

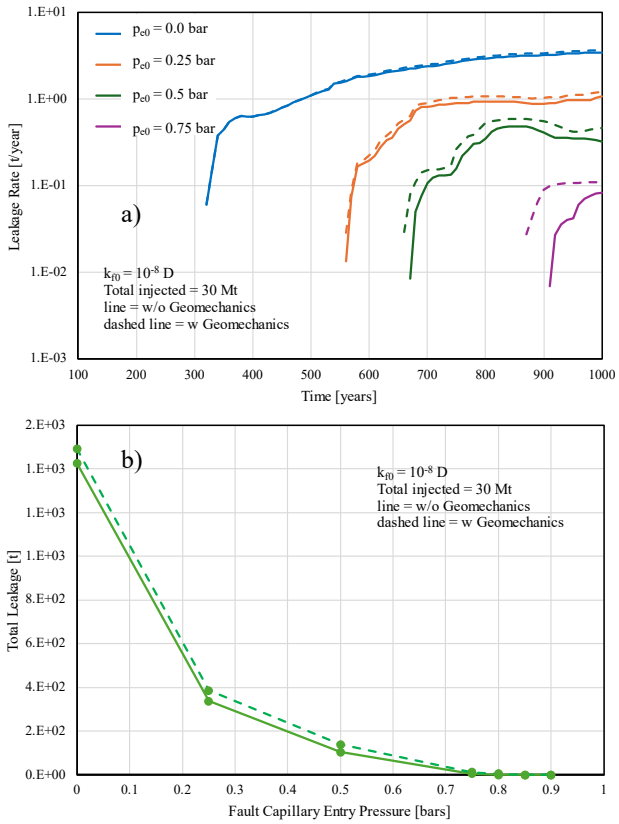

Fig. 5. Impact of fault capillary entry pressure on CO_2 leakage showing the leakage profile for different fault capillary entry pressures where higher entry pressures act as a barrier, delaying and reducing the CO_2 leakage and no leakage occurs for a scenario of 0.9 bar entry pressure (a) and the decrease in total CO_2 leakage with increasing value for fault capillary entry pressure (b) for simulations with and without incorporating geomechanics.

4. CONCLUSIONS

This study presents an efficient computational tool for simulating fault leakage in CO_2 storage applications incorporating uncertainty. The approach integrates an upscaled fault leakage function with geomechanical constraints into a VE reservoir modeling framework, addressing the challenge representing complex fault

structures during early storage site screening when data is limited. The method's computational efficiency enables rapid assessment of numerous geological scenarios, facilitating the identification of promising storage projects and guiding targeted data acquisition. Application to various CO_2 injection scenarios provided insights into key factors influencing along fault leakage. While the current model assumes constant fault properties, future work could explore the incorporation of more detailed, stochastic representations of fault hydraulic properties and realistic geomechanical constraints to improve the model reliability and applicability.

REFERENCES

Abd Rahman, I. Z., Abang Hasbollah, D. Z., Mohd Yunus, N. Z., Kasiman, E. H., & Mazlan, A. N. (2022). Carbon dioxide storage potential in malaysian sandstone aquifer: An overview. *IOP Conference Series: Earth and Environmental Science*, *971*(1), 012022. https://doi.org/10.1088/1755-1315/971/1/012022

Andersen, O. (2017). *Simplified models for numerical simulation of geological CO2 storage* [Doctoral thesis, The University of Bergen]. https://bora.uib.no/bora-xmlui/handle/1956/15477

de Jonge-Anderson, I., Ramachandran, H., Nicholson, U., Geiger, S., Widyanita, A., & Doster, F. (2024a). Determining CO2 storage efficiency within a saline aquifer using reduced complexity models. *Advances in Geo-Energy Research*, *13*(1), 22–31. https://doi.org/10.46690/ager.2024.07.04

de Jonge-Anderson, I., Widyanita, A., Busch, A., Doster, F., & Nicholson, U. (2024b). New insights into the structural and stratigraphic evolution of the Malay Basin using 3D seismic data: Implications for regional carbon capture and storage potential. *Basin Research*, 36(4), e12885. https://doi.org/10.1111/bre.12885

Espinoza, D. N., & Santamarina, J. C. (2017). CO2 breakthrough—Caprock sealing efficiency and integrity for carbon geological storage. International Journal of Greenhouse Gas Control, 66, 218–229. https://doi.org/10.1016/j.ijggc.2017.09.019

Gasda, S., Keilegavlen, E., Sandve, T. H., Berge, R., Pettersson, P., & Krumscheid, S. (2022). Practical field-scale simulation approaches for quantification of fault-related leakage under uncertainty. *SSRN Electronic Journal*. https://doi.org/10.2139/ssrn.4277020

Hasbollah, D. Z. A., Junin, R., Taib, A. M., & Mazlan, A. N. (2020). Basin evaluation of co2 geological storage potential in malay basin, malaysia. In P. Duc Long & N. T. Dung (Eds.), *Geotechnics for Sustainable Infrastructure Development* (Vol. 62, pp. 1405–1410). Springer Singapore. https://doi.org/10.1007/978-981-15-2184-3_184

Kang, M., Nordbotten, J. M., Doster, F., & Celia, M. A. (2014). Analytical solutions for two-phase subsurface flow to a leaky fault considering vertical flow effects and fault properties. *Water Resources Research*, *50*(4), 3536–3552. https://doi.org/10.1002/2013WR014628

Knipe, R. J., Jones, G., & Fisher, Q. J. (1998). Faulting, fault sealing and fluid flow in hydrocarbon reservoirs: An introduction. *Geological Society, London, Special Publications*, *147*(1). https://doi.org/10.1144/GSL.SP.1998.147.01.01

Krevor, S., De Coninck, H., Gasda, S. E., Ghaleigh, N. S., De Gooyert, V., Hajibeygi, H., Juanes, R., Neufeld, J., Roberts, J. J., & Swennenhuis, F. (2023). Subsurface carbon dioxide and hydrogen storage for a sustainable energy future. *Nature Reviews Earth & Environment*, *4*(2), 102–118. https://doi.org/10.1038/s43017-022-00376-8

Lie, K.-A. (2019). *An introduction to reservoir simulation using matlab/gnu octave: User guide for the matlab reservoir simulation toolbox(Mrst)* (1st ed.). Cambridge University Press. https://doi.org/10.1017/9781108591416

Malaysian Continental Shelf Project, National Security Council, Malaysia, Madon, M., Jong, J., & JX Nippon Oil and Gas Exploration (Malaysia) Limited, Malaysia. (2021). Geothermal gradient and heat flow maps of offshore malaysia: Some updates and observations. Bulletin of the Geological Society of Malaysia, 71, 159–183. https://doi.org/10.7186/bgsm71202114

Manzocchi, T., Childs, C., & Walsh, J. J. (2010). Faults and fault properties in hydrocarbon flow models. *Geofluids*, *10*(1–2), 94–113. https://doi.org/10.1111/j.1468-8123.2010.00283.x

Neufeld, J. A., Vella, D., & Huppert, H. E. (2009). The effect of a fissure on storage in a porous medium. *Journal of Fluid Mechanics*, *639*, 239–259. https://doi.org/10.1017/S0022112009991030

Nordbotten, J. M., & Celia, M. A. (2011). *Geological storage of co2: Modeling approaches for large-scale simulation* (1st ed.). Wiley. https://doi.org/10.1002/9781118137086

Ramachandran, H., Jonge-Anderson, I. de, Musa, I. H., Nicholson, U., Tan, C. P., Geiger, S., & Doster, F. (2024). *Rapid fault leakage modeling for co2 storage in saline aquifers*. https://eartharxiv.org/repository/view/7535/

Rizzo, R. E., Inskip, N. F., Fazeli, H., Betlem, P., Bisdom, K., Kampman, N., Snippe, J., Senger, K., Doster, F., & Busch, A. (2024). Modelling geological CO2 leakage: Integrating fracture permeability and fault zone outcrop analysis. *International Journal of Greenhouse Gas Control*, *133*, 104105. https://doi.org/10.1016/j.ijggc.2024.104105

Snippe, J., Kampman, N., Bisdom, K., Tambach, T., March, R., Maier, C., Phillips, T., Inskip, N. F., Doster, F., & Busch, A. (2022). Modelling of long-term along-fault flow of CO2 from a natural reservoir. *International Journal of Greenhouse Gas Control*, *118*, 103666. https://doi.org/10.1016/j.ijggc.2022.103666

Yortsos, Y. C. (1995). A theoretical analysis of vertical flow equilibrium. *Transport in Porous Media*, *18*(2), 107–129. https://doi.org/10.1007/BF01064674

Zheng, X., & Espinoza, D. N. (2022). Stochastic quantification of CO2 fault sealing capacity in sand-shale sequences. *Marine and Petroleum Geology*, *146*, 105961. https://doi.org/10.1016/j.marpetgeo.2022.105961